Diyala Journal of Engineering Sciences

Journal homepage: https://djes.info/index.php/djes

ISSN: 1999-8716 (Print); 2616-6909 (Online)

Study the Effect of Adding Heat Exchanger on the Refrigeration System Performance

Maytham Neamah Jasim*, Yaser Alaiwi

Department of Mechanical Engineering, Altinbaş University, Istanbul 34217, Turkey

ARTICLE INFO

Article history:
Received November 12, 2022
Revised April 7, 2023
Accepted April 10, 2023
Available online April 15, 2023

Keywords:
Shell and tube
Coefficient of performance (COP)
Engineering Equation Solver (EES)
Condenser
Subcooling

ABSTRACT

Internal, or liquid-suction, heat exchangers are used with the primary goal of ensuring the entry of refrigerant in the liquid phase to the expansion device. The greatest COP gain is primarily determined by the thermodynamic parameters linked to the relative increase in refrigerating effect. Large latent heat of vaporization refrigerants often does not gain as much from condenser subcooling in support of a cooling system. Computational fluid dynamics (CFD) is used to study the effects of the turbulence model, which requires the solution of two transport equations. A technique was developed to study the thermal effect on the heat exchange process between two fluids. To observe the temperature effect on 17 tubes, the diameter was altered twice, first to 6 mm and then to 4 mm. The flow procedure happened in one direction, and the tube that contains the tubes had a diameter of 50 mm. The best-case scenario is the case where the pipe diameter is 4 mm and the heat exchanger are 300 mm in length. Through the results, the enthalpy was improved in the simulated cases to 423.2 h [KJ/M]. The length of the heat exchanger greatly affects the values of the exit temperatures and the temperature difference. For a length of 225 mm, the temperature reached 15.73 °C, and for 300 mm, it reached 13.847 °C. The significant reduction in temperatures helps increase the coefficient in the refrigeration cycle. A high coefficient of cooling in the heat exchanger appears when the length is 300 mm compared to other lengths.

1. Introduction

An in-depth analysis of the R1234yf and R134a refrigerants' inner intensity exchanger's intensity-movement characteristics Under operational conditions, the relationship between COP and the general intensity move coefficient, as well as the effects on the heat exchanger's length and efficiency, annular space, and strain drop, were examined. The huge annular area of the internal heat exchangers will often result in unfavorable intensity movement coefficients because laminar streams through the annular region are not suitable for increasing COP. [1].

LSHX and R290 have enormous financial potential as a replacement for current systems in the future due to their low potential for unnatural weather change and nearly identical refrigerant characteristics to those of R22, R410A, R290, and R32. An examination of subcooling using a fluid pull heat exchanger (LSHX) on the display of a cooling framework using these refrigerants. [2]. The temperature at the condenser outlet decreased by 2.2 °C as a result of the reduced blower release pressure. The cooling capability of the split-type climate control system is 2.5 kW. [3].

The majority of coolers use a fume pressure cycle (VCC), which considers their other

* Corresponding author.
E-mail address: neamahmaytham@gmail.com
DOI: 10.24237/djes.2023.16201

available possibilities. We looked at three classes: multi-stage cycles, development misfortune recovery cycles, and double evaporator cycles. The use of private coolers is shown to use non-VCC advancements. These include advancements in thermoelastic, thermoelectric, attractive, and thermoacoustic technologies. [4]. The IHX's maximum amount of entropy was taken into account while recreating the framework. For both R152a and R134a, the maximum entropy age occurs at 66 percent viability. The framework was determined to operate at its best practicable level when the R1234ZE refrigerant was used. For each occurrence, the effects of subcooling and superheating are assessed. [5].

The internal regenerative heat exchange mechanism of a closed-loop cooling system recovers important cooling and heating energy. The best recovery techniques include regenerative heat exchangers, which are comparable to the pull-line heat exchanger seen in fume pressure frameworks. Each of the three recovery techniques is shown with its actual implementation, a review of its continuing level of development, and appraisals of its benefits, drawbacks, and distinguishing characteristics. [6]. The findings demonstrated that the hot stream was primarily impacted by the transient shift caused by the supercritical operating conditions. The shift in mass stream rate causes a decrease in the intensity move rate and warm viability at the start of the framework's activity. The transient behavior of the presentation coefficient has a backward connection with the warm sufficiency of the inner heat exchanger. [7]. The cooling limit of R1234ze(E) is expanded to the same extent as R134a by using an open-type blower that is 43 percent larger and an interior heat exchanger that is 25 percent more efficient. For R450A, it essentially has to be started using IHX. Unadulterated hydrofluoroolefins (HFOs), unsaturated organic molecules made of carbon, fluorine, and hydrogen, were recommended as a replacement for this liquid; nonetheless, framework adjustments are often anticipated to achieve appropriate execution. [8]. R1234yf is used as a drop-in replacement for R134a in the experimental study for three household refrigerators that are identical to those in this work. Compared to R134a, this leads to a little increase in energy consumption of 4%. TEWI research finally revealed that it was 1.07 percent more expensive than R-134a. [9]. In steady state settings with subcooling temperatures, evaporators with R290 or R600a may achieve -30 °C. R404a and R22 lower may achieve -24 and -22 °C, respectively. R290 and R600a, which may be combined 50/50, have qualities that are comparable to those of R404A and might be used as a replacement. 3.91 percent, 7.78 percent, and 11.87 percent, respectively, were the usual RCI increases [10]. The R1234yf framework has a 4.0–7.0% lower cooling limit and a 3.6-4.5% COP. For a blower speed of 800–1800 rpm, the COP is 0.3–2.9 percent lower than that of the R134a framework. With and without the IHX, the second regulation effectiveness of R12 34 YF was expanded by 1.5–4 %. At all blower speeds, the EDR (energy destruction ratio) of the framework was 0.5–3.3% [11].

Only low-GWP refrigerants will be allowed in wealthy nations in the medium future. One of the most promising among them is R1234ze. The majority of HVACR applications may employ this refrigerant because to its strong environmental attributes. When combined with other refrigerants, the final GWP value is also significantly reduced [12]. As condenser subcooling increases, the tradeoff between growing refrigerating effect and specific pressure work causes the COP to reach an extreme. Due to the thermodynamic limits associated with the general expansion in refrigerating effect, i.e., fluid explicit intensity and idle intensity of vaporization, the greatest COP increase is still up in the air [13]. An overview of several improvements and enhancement techniques for a fume pressure refrigeration cycle-based vehicle temperature control system is provided in this article. This essay primarily consists of two sections. The first is a study of how to make the auto cooling (AAC) framework's mandatory and optional components more efficient. The second looks at how well functional administration and control use energy to operate the AAC system [14].

The study's objective is to use refrigeration cycles to implement heat recovery concepts in HVAC applications. It focuses on how energy recovery relates to the areas of heating, ventilation, and air conditioning. The condenser's lost energy is used to heat or pre-heat household water. Thermal modeling for the whole system is produced, and a corresponding iterative code is shown. The outputs of calculations utilizing the code offer magnitude orders for energy management and savings [15]. The R1234YF mobile air conditioning (MAC) system's potential for performance improvement was investigated using thermodynamic cycle analysis. We looked at the effects of compressor coefficient, subcooling at the condenser outlet, and superheat at the evaporator outlet. It was determined that the benefits of superheat for cooling capacity and system coefficient of performance were negligible (COP). The compressor's isentropic coefficient had a substantial role in the rise in system COP. The compressor coefficient should be increased, and an internal heat exchanger should be installed, as the two best options for the following MAC system modification. [16].

Erosion coefficients for nano-oil with a convergence of 1-3 g/L are 12.9–19.6% lower than for pure mineral oil. It has been tested how long nanoparticles may stay suspended in mineral oil under fixed conditions. The grating coefficients of the nano-oil dramatically decrease as there are more nanoparticles in the mineral oil, particularly at lower applied loads [17]. Both household and commercial buildings often use split-type air conditioners (A/Cs). To save a lot of energy, the appearance of this A/C might be enhanced. An ejector might be used in conjunction with temperature control systems to increase COP. The mathematical results shown that, individually, spout and blending chamber diameters of 1.1- and 2.5-mm result in the perfect COP improvement. Separate increases in COP of 4.17, 11.14, and 13.78 percent have been observed for the modified ejector cycle at surrounding temperatures of 30, 35, and 40 °C [18].

The energy coefficient and relative CO2 emissions of two R134a drop-in replacements with low global warming potential (COP) were studied. Three characteristics were looked at: COP, cooling capacity, and volumetric coefficient. Various evaporation and condensation temperature values were mixed during tests in a vapor compression system under observation. The COP fluctuations between the two replacements are minimized by using an internal heat exchanger [19]. A numerical method has been suggested for determining the motive nozzle and constant-area of an ejector used as an expansion device. When installing split-type air conditioners in locations with moderate to high outside air temperatures, capillary tubes are often used. The results demonstrated that despite temperature changes, the ejector's diameter (1.14 mm) remained consistent [20].

In this work, supercritical CO2 microtube heat exchangers composed of the superalloy Haynes 282 are optimized using a 2D numerical shell-and-tube heat exchanger performance prediction model. These heat exchangers are improved via particle swarm optimization, producing small and affordable designs with power densities around 20 kW/kg and costs per conductance around $5 K/W [21].

In this work, shell and tube heat exchangers with round and hexagonal tubes operating in both parallel and counter-flow configurations at different flow velocities were investigated experimentally. The heat transfer rate, temperature drop, and heat transfer coefficient were calculated using three turbulence models (SST). When CFD is used for counter and parallel flow, it has been shown that the rate of heat transfer is related to fluid velocities and the number of tubes turns. The flow in hexagonal tubes may be disturbed more readily than in round tubes, which increases the rate of heat transfer [22]. It has cooling capacity and heat rejection. It is not one of the objectives of the research, the objectives of the research are limited to knowing the coefficient of cooling by adding heat exchangers with variable designs.

2. Methodology

In order to obtain accurate results, it was necessary to combine two programs to complete the understanding of the results obtained, as the ANSYS program studies the heat exchanger and

the method of heat transfer in it. As for the EES, it works by drawing a cycle diagram for the refrigeration system and showing the properties.

2.1 General Mass, Energy, and Exergy Equations of EES

The conservation of mass equation for system [23] :

$$\sum \dot{m}_{in} = \sum \dot{m}_{out} \quad (1)$$

where: $\sum \dot{m}_{in}$: the total mass flow entering the system per unit time, $\sum \dot{m}_{out}$: the total mass flow exiting the system per unit time.

The energy balance for each component is based on the first law of thermodynamics for system [23]:

$$\dot{Q} + \dot{W} = \sum \dot{m}_{out} h_{out} - \sum \dot{m}_{in} h_{\text{in}} \quad (2)$$

where: $\dot{Q}$: The heat transfer per unit time, $\dot{W}$; Work done by the control volume per unit time, h_{in} : Specific enthalpy per the mass entering the system.

h_{out}: Specific enthalpy per mass leaving the system.

Unlike mass and energy, entropy is not conserved in open and closed systems, as entropy is produced due to irreversibility. In open systems, the entropy balance can be expressed as:

$$\dot{E} = \dot{m}\psi \quad (3)$$

$$\text{COPcooling} = \frac{T_{\text{COLD}}}{T_{\text{HOT}} - T_{\text{COLD}}} \quad (4)$$

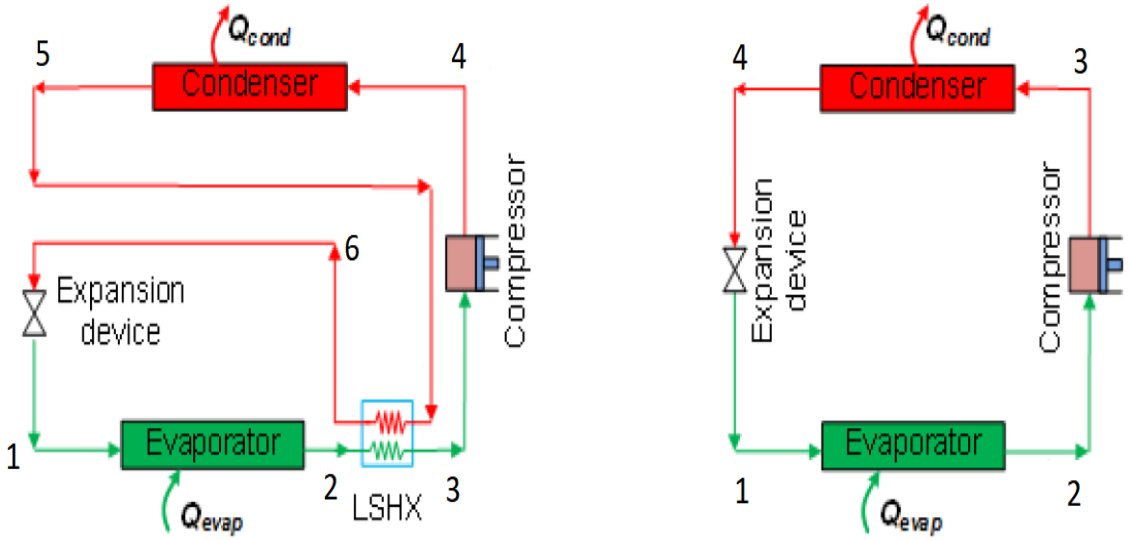

Figure 1. Schematic diagrams of a vapor compression refrigeration cycle. (a) Cycle with LSHX (b) Basic cycle.

2.2 Computational analysis using ANSYS package

Studies in computational fluid dynamics (CFD) are conducted to get more knowledge about the flow. A model of k-e is used to highlight the impact of the turbulence model by solving a two-transport equation. Therefore, these cartesian coordinate systems may be solved using numerical solution methods (x, y, and z). The geometry in three dimensions is produced.

ANSYS version 19 will be implemented here to generate the system geometry, grid it, and run the simulations.

2.2.1 Assumptions

In the current study, R140A is considered as the running liquid and the characteristics of flow are assumed to be:

- Steady flow, three dimensional,
- Newtonian,
- Incompressible, and
- Turbulent.

2.2.2 Governing equations

The governing equations to be solved are the continuity, momentum and the equation of the energy.

- Mass Conservation (Continuity) [23]

Mass conservation is expressed mathematically as the continuity equation, which relates the rate of mass flow into and out of a control volume to the change in mass within the volume. The continuity equation is derived from the principle of conservation of mass.

$$\nabla \cdot (V) = 0 \tag{5}$$

- Momentum Equation [23]

$$\nabla \cdot (\rho \dot{V} \dot{V}) = -\nabla p + \nabla \cdot (\bar{\tau}) \tag{6}$$

The stress tenser $\bar{\tau}$ is given by [23]:

$$\bar{\tau} = \mu \left[\left(\nabla \vec{V} + \nabla \vec{V}^T \right) - \frac{2}{3} \nabla \cdot \vec{V} I \right] \tag{7}$$

- Energy Equation [23]**:**

$$\nabla \cdot (\dot{V}(\rho E)) = \nabla (k \nabla T - \rho C \dot{V} T') \tag{8}$$

- Turbulence Equations

To account for the existence of robust matter, sinks have been included into all of the disturbance situations in the mellow and stable regions. Similar to the force sink word, the sink phrase has the following form:

$$S = \frac{(1-\beta)^2}{(\beta^2+\varepsilon)} A_{mush} \varphi \tag{9}$$

where φ the mushy zone constant (k, ε, ω, and so on) and represents the turbulence quantity being addressed A_{muss} .

2.2.3 System geometry

The system architecture shown in Figure 2 consists of a shell and tube type heat exchanger with variable lengths to see the thermal effect in the heat exchange process between the two fluids. Three different lengths were taken: 150 mm, 225 mm, and 300 mm. As for the diameter of the tubes, it was changed twice, once to 6 mm and once to 4 mm, to see the thermal effect and the number of tubes (17). Also, the tube containing the small tubes has a diameter of 50 mm, and the flow process was the opposite way.

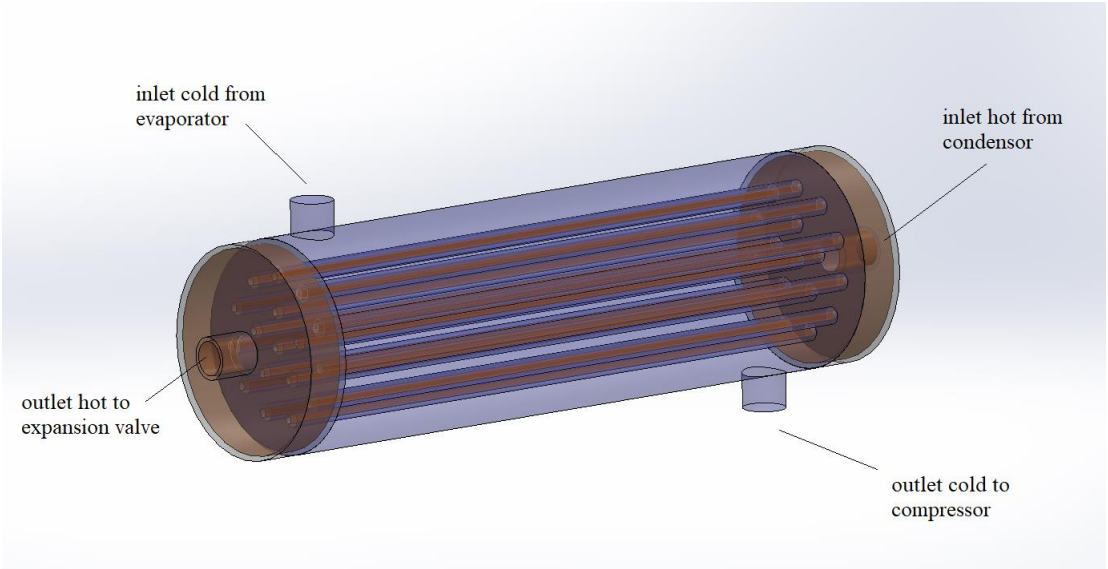

Figure 2. Geometry shape

2.2.4 *Mesh generation*

Since unstructured grids tend to work well for complicated geometries, a tetrahedron grid was employed in this investigation. In ANSYS, users just need to provide input in a single phase to generate a mesh for a solid geometry or a 3D model. In this work, a total of (8383882) cells were collected, see fig (3).

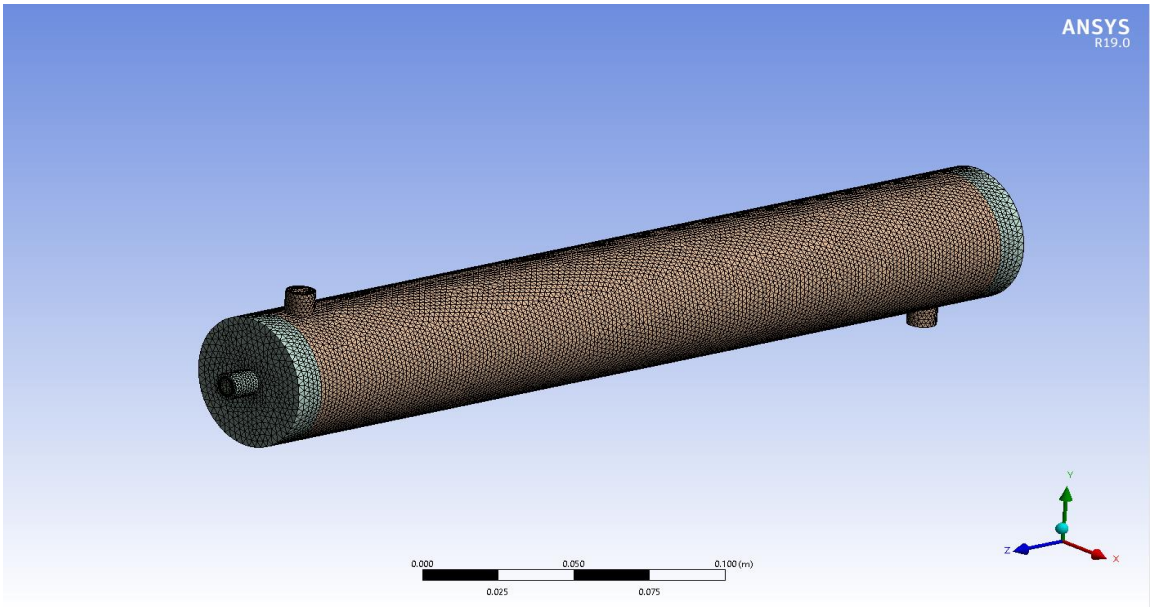

Figure 3. Mesh generated

Table 1: Mesh independency

Case	Number of elements	Max. temperature (°C)
1	2742012	55.253
2	4624300	53.911
3	6457344	53.871
4	8383882	53.863

2.2.5 *Conditions of the boundary*

Where the pressures and temperatures extracted from the EES program (table 2) were entered as the results sources for the CFD program, which is considered a boundary condition. The EES program that finds cycle variables in the form of exact equations based on the ASHRAE source. The required capacity of the compressor is 10,033 Btu/hr (0.83 tons).

Table 2: Boundary conditions of EES

point	P [bar]	T [C]
1	678.3	-5.081
2	678.3	-5
3	932.5	4.975
4	1889	52.89
5	1889	30
6	1531	22.06

2.2.6 *Initial conditions*

Since the flow field can't be determined until after iteration has begun, a best estimate is required before any progress can be made toward a solution. All parameters in this study are set relative to the inlet boundary conditions of the inner pipe.

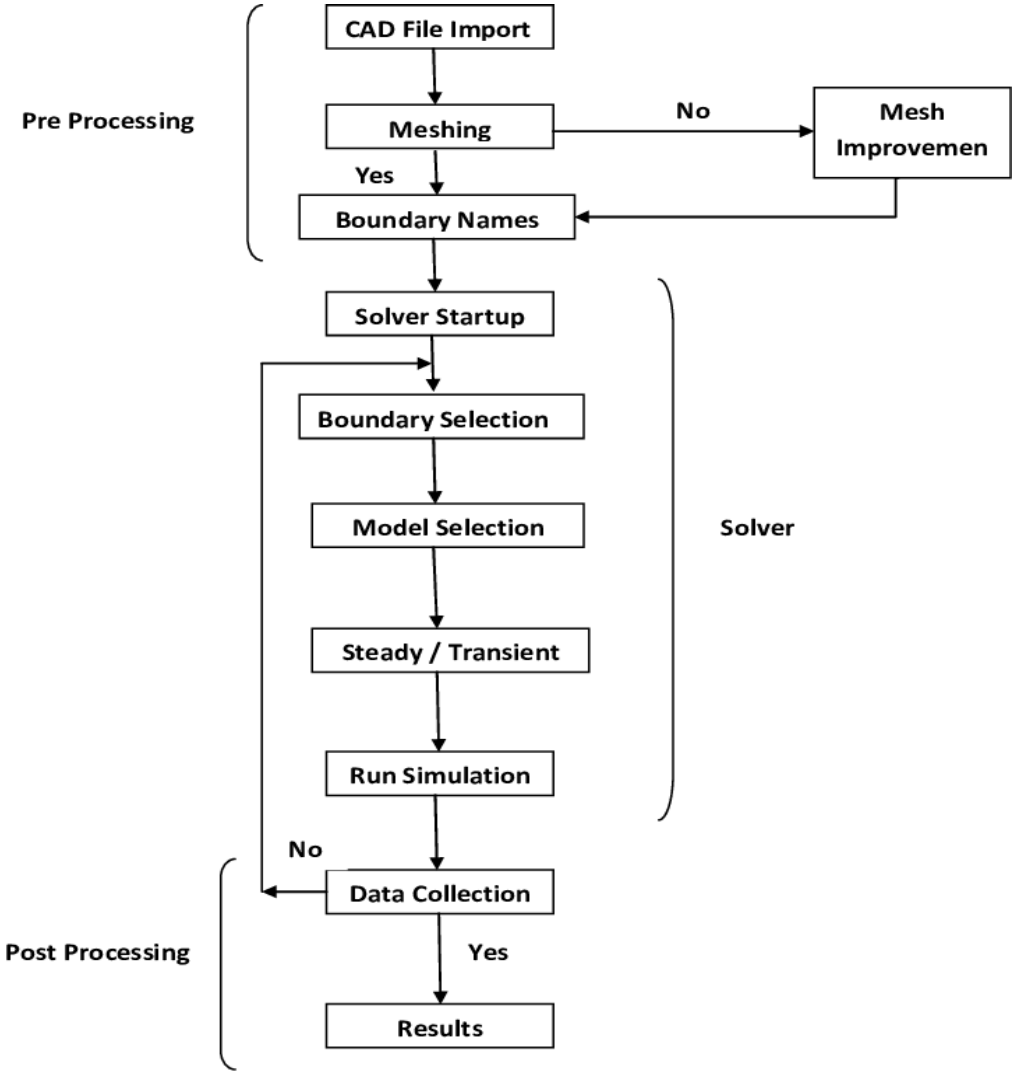

Figure 4. Flow chart of simulation

3. Results and discussion

3.1 Effect of heat exchanger tube diameter on the refrigeration cycle

The diameter of the heat exchanger for the manufactured tubes has a significant impact on the refrigeration value of the gas coming from the condenser, which has relatively high temperatures. Through the results obtained with regard to changing the diameter of the inner tube, it is possible to notice an increase in the cycle enthalpy at point 3. as shown in Table 3. Through Table 3, the composition of the refrigeration cycle is observed by the axes represented by the cycle as temperatures and the entropy of the cycle through the data mentioned in the numerical work.

Table 3: The results obtained from the EES program without heat exchanger

point	h [kJ/M]	P [bar]	s [J/K]	T [C]	X	V
1	248.3	678.3	1.181	-5.075	-	0.0101
2	419.8	678.3	1.82	-5	1	0.03852
3	462.9	1889	1.867	58.4	-	0.01636
4	248.3	1889	1.164	30	0	0.000967

Figure 5 shows the thermal effect in the heat exchanger and the method of transferring thermal energy according to the diameter of the tubes in the heat exchangers. As the heat exchange process for the hot outlet, the temperature value is greater at the tube diameter of 6 mm, where the outlet temperature was 23.577 °C. As for the diameter of 4 mm, the temperature returns of the outlet reached 22.056 °C. The cooling coefficient of the heat exchanger is better when the tube diameter is 4 mm. To ensure the accuracy of the readings, the COP value is obtained through the EES program. This case reached 5.044 at a diameter of 4 mm, and at a diameter of 6 mm, it reached 4.864. Where it gives more confirmation that the case in which the heat exchanger of 4 mm is better compared to the other diameter.

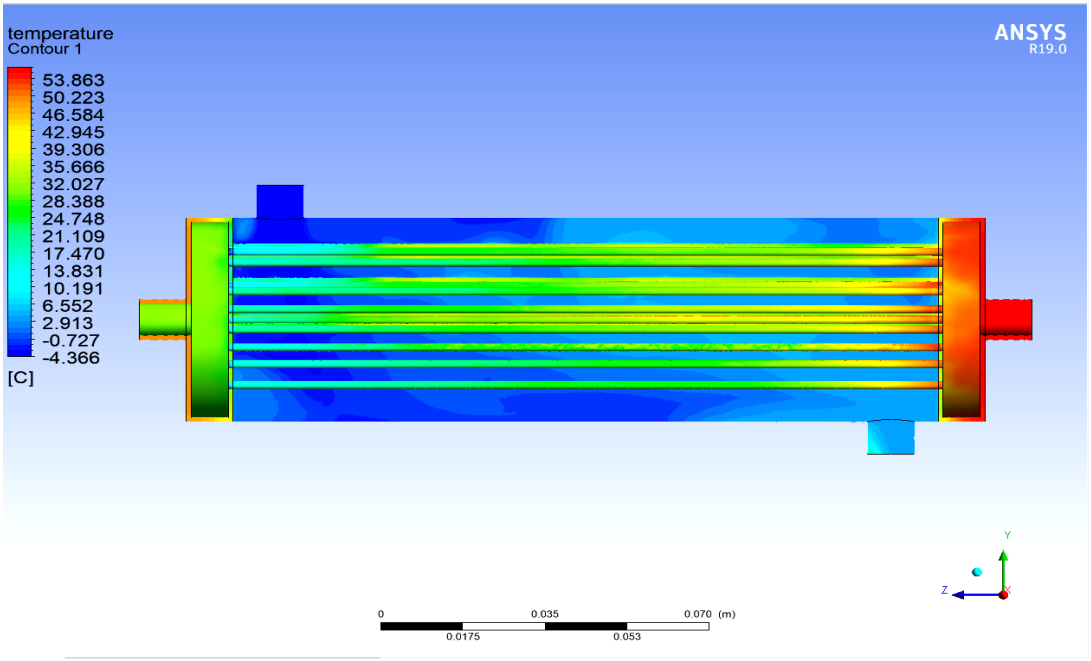

(a)

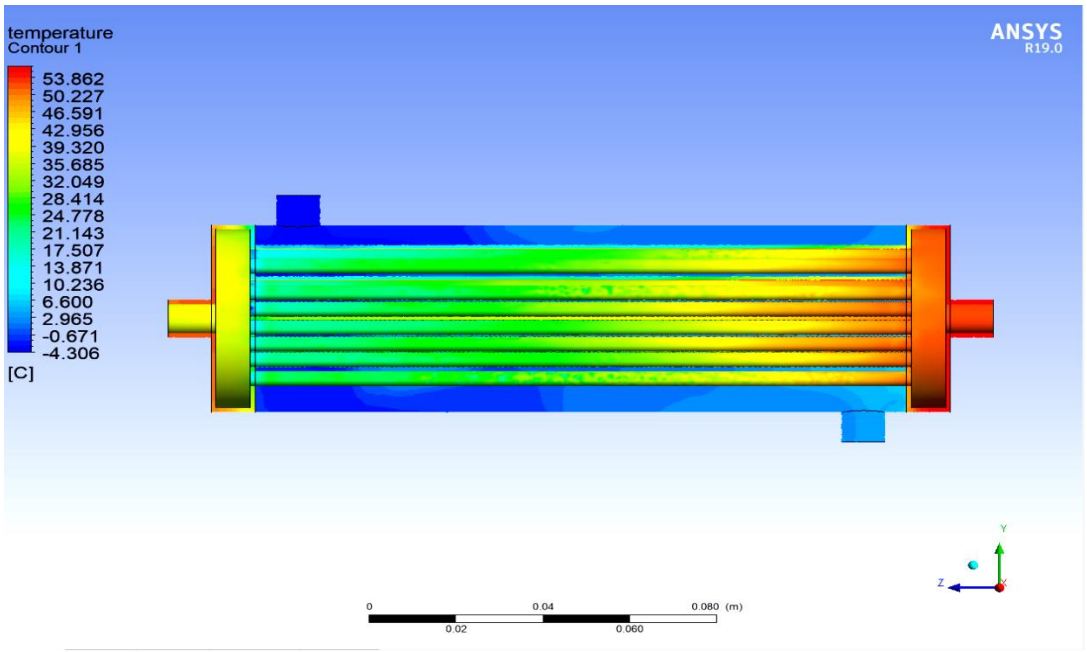

(b)

Figure 5. Temperature contour of heat exchanger (shell and tube) at pipe diameter (a) 4 mm, (b) 6 mm.

Since the cooling process in the heat exchanger was better in terms of diameter (4 mm), this can be confirmed by the COP value; this value increases the coefficient of the cooling system. This is evident from Figure 4.3, as the shape of the cycle varies according to the diameter of the pipes, and point 4 increased significantly with the value of temperature and entropy. The case was 4 mm better compared to a 6 mm pipe diameter, as shown in tables 4 and 5.

Table 4: The results obtained from the EES program when the tube diameter is 4 mm, the number of tubes is 17, and the length of the heat exchanger is 150 mm.

point	h [kJ/M]	P [bar]	s [J/K]	T [C]	X	V
1	234.8	678.3	1.131	-5.081	-	0.007877
2	419.8	678.3	1.82	-5	1	0.03852
3	422.8	932.5	1.801	4.975	1	0.0279
4	456.5	1889	1.847	52.89	-	0.01579
5	248.3	1889	1.164	30	0	0.000967
6	234.8	1531	1.12	22.06	0	0.000931

Table 5: The results obtained from the EES program when the tube diameter is 6 mm, the number of tubes is 17, and the length of the heat exchanger is 150 mm.

point	h [kJ/M]	P [bar]	s [J/K]	T [C]	X	V
1	237.4	678.3	1.14	-5.08	-	0.008296
2	419.8	678.3	1.82	-5	1	0.03852
3	422.5	896.4	1.803	3.697	1	0.02906
4	457.3	1889	1.85	53.6	-	0.01587
5	248.3	1889	1.164	30	0	0.000967
6	237.4	1595	1.129	23.58	0	0.000938

Through the attached tables, it is noted that the enthalpy value at point 3, represented by the outlet of the cold heat exchanger coming from the evaporator, is higher in the case where the tube diameter is 4 mm, as it was 422.8 KJ/M, which is higher than the case where the tube diameter is 6 mm.

3.2 Effect of heat exchanger tube length on the refrigeration cycle

The increase in the length of the heat exchanger greatly affects the value of the exit temperatures and the temperature difference. Figure 6 shows the effect of the length of the heat exchanger on the temperatures, and thus the significant reduction in temperatures helps to increase the coefficient in the refrigeration cycle. As Figure 6.

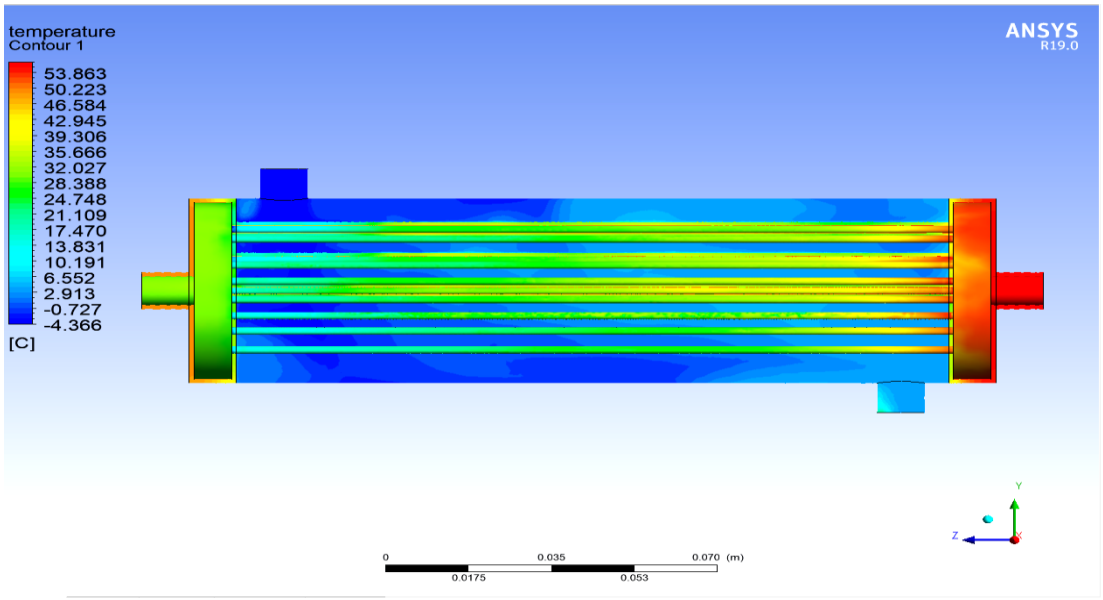

(a)

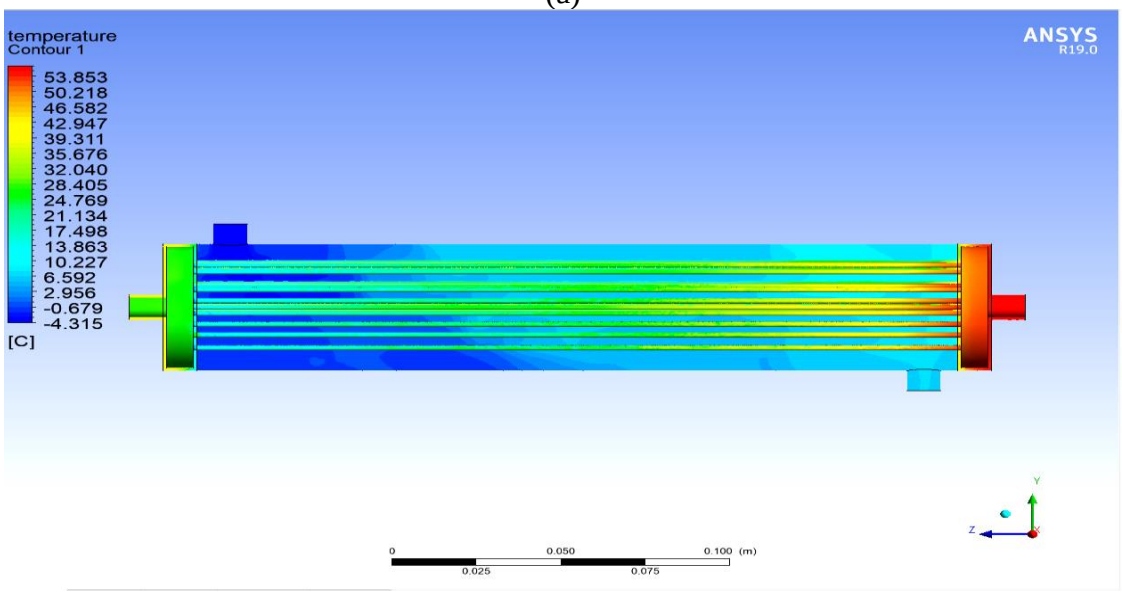

(b)

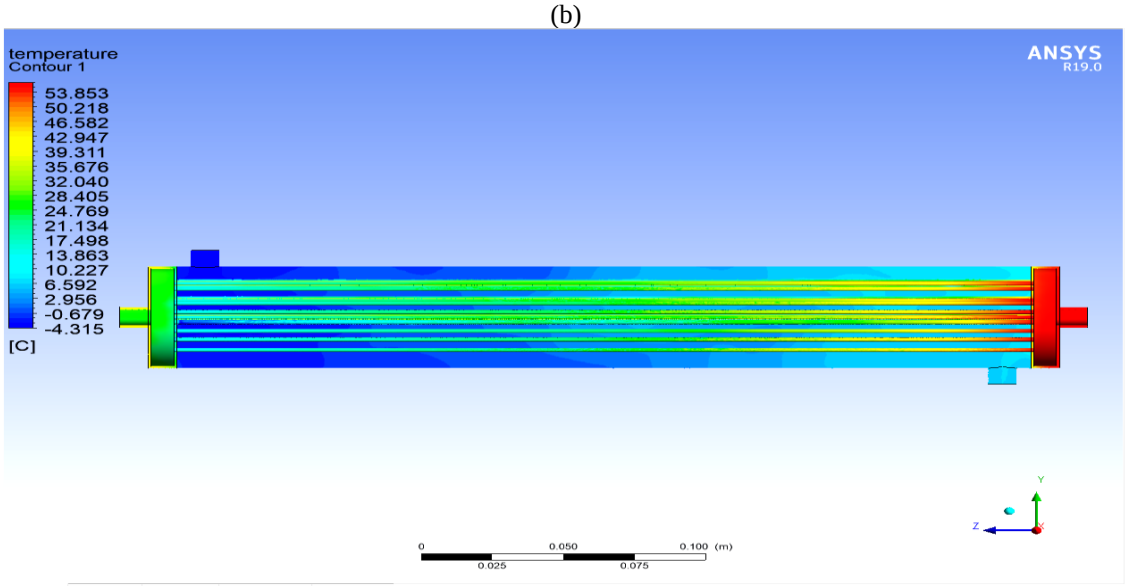

(c)

Figure 6. Temperature contour of heat exchanger (shell and tube) at pipe length (a) 150 mm, (b) 225 mm, (c) 300 mm.

Where the figure shows the significant decrease in the exit temperatures with the increase in the length of the heat exchanger, the exit temperature of the heat exchanger on the hot side represented by the condenser reached 22.056 °C for a length of 150 mm with a diameter of 4 mm. As for the length of 225 mm, the temperature reached 15.73 °C, and for the length of 300 mm, it reached 13.847 °C. Where the high coefficient of cooling in the heat exchanger appears when the length of the heat exchanger is 300 mm compared to other lengths.

As shown in tables 6, 7, and 8, and through the relationship between temperature and entropy, the difference in the cycle temperature values is noticed, as the value of point 4 decreases with the increase in the temperature difference, i.e., the increase in the length of the heat exchanger. Thus, the best condition is reached when the length of the heat exchanger is 300 mm.

Table 6: The results obtained from the EES program when the tube diameter is 4 mm, the number of tubes is 17, and the length of the heat exchanger is 150 mm.

point	h [kJ/M]	P [bar]	s [J/K]	T [C]	X	V
1	234.8	678.3	1.131	-5.081	-	0.007877
2	419.8	678.3	1.82	-5	1	0.03852
3	422.8	932.5	1.801	4.975	1	0.0279
4	456.5	1889	1.847	52.89	-	0.01579
5	248.3	1889	1.164	30	0	0.000967
6	234.8	1531	1.12	22.06	0	0.000931

Table 7: The results obtained from the EES program when the tube diameter is 4 mm, the number of tubes is 17, and the length of the heat exchanger is 225 mm.

point	h [KJ/M]	P [bar]	s [J/K]	T [C]	X	V
1	224.5	678.3	1.092	-5.086	-	0.00617
2	419.8	678.3	1.82	-5	1	0.03852
3	423.2	979.4	1.798	6.586	1	0.02653
4	455.4	1889	1.844	52	-	0.0157
1	248.3	1889	1.164	30	0	0.000967
6	224.5	1285	1.086	15.73	0	0.000906

Table 8: The results obtained from the EES program when the tube diameter is 4 mm, the number of tubes is 17, and the length of the heat exchanger is 300 mm.

point	h [kJ/M]	P [bar]	s [J/K]	T [C]	X	V
1	221.5	678.3	1.081	-5.087		0.005671
2	419.8	678.3	1.82	-5	1	0.03852
3	423.2	978.4	1.798	6.552	1	0.02656
4	455.4	1889	1.844	52.01		0.0157
5	248.3	1889	1.164	30	0	0.000967
6	221.5	1217	1.076	13.85	0	0.0009

Through the previous tables represented by the results obtained through the EES program, which show the preference of the length of the heat exchanger with 300 mm over the rest of the first, and through the enthalpy used at point 3, represented by the exit of the evaporator, whose value is 423.2 kJ/M, at point 6, represented by the exit, the condenser decreased to 221.5 kJ/M.

3.3 Effect of heat exchanger length and tube diameter on COP

The exit temperature of the heat exchangers decreases as the value of the length of the heat exchangers increases, which thus increases the coefficient of performance (COP) of the cooling system. In Figure 6, it is noted that the value of the hot temperatures decreases dramatically with an increase in the length of the heat exchanger and that the opposite behavior occurs on the cold side. In addition, the best COP reached is 5.566 in the case where the length of the heat exchanger is 300 mm and the diameter of the tubes is 4 mm.

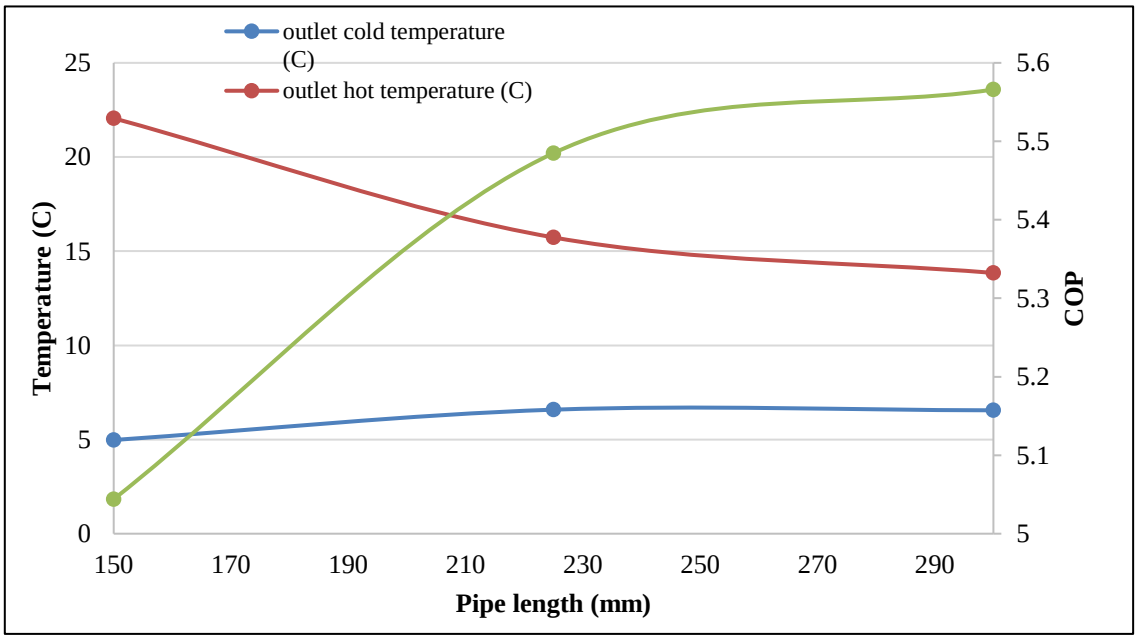

Figure 7. COP and temperature with pipe length at 4 mm dimeter pipe

As for the pipe diameter of 6 mm in Figure 8, we notice the same features, namely, that the increase in the length of the heat exchanger decreases the value of the exit temperatures for the hot side. Where the COP value at the diameter of 6 mm reached 5.24 at the length of the heat exchanger of 300 mm, which is lower compared to the diameter of 4 mm.

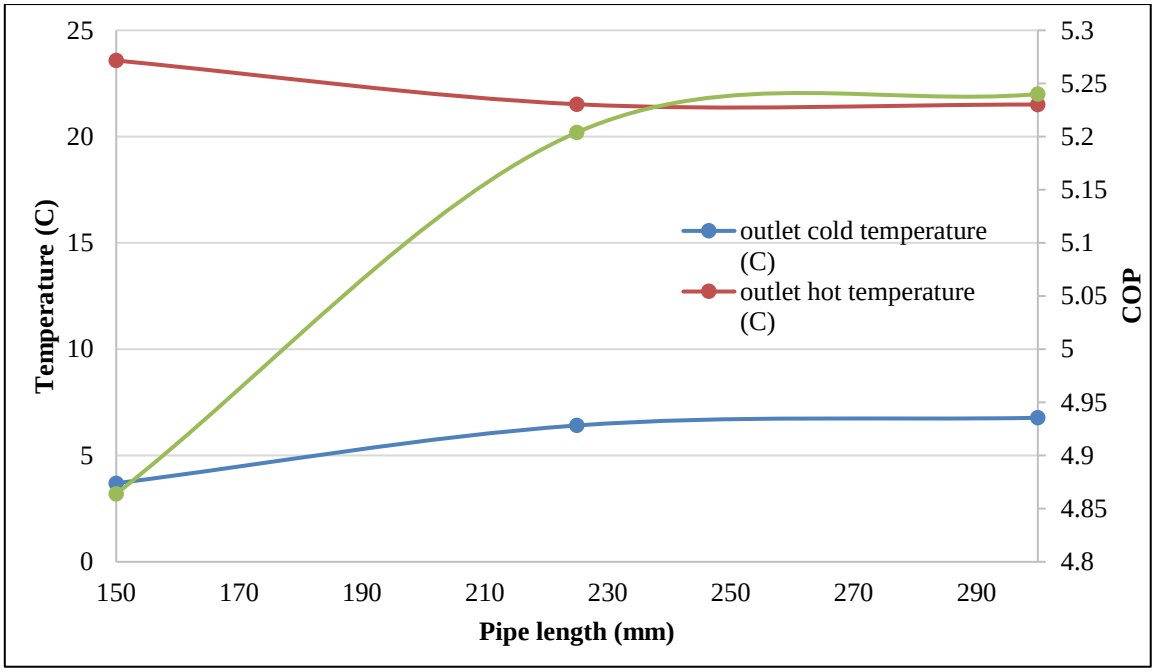

Figure 8. COP and temperature with pipe length at 6 mm dimeter pipe

Table 9 represents the exit temperatures of the heat exchanger and the performance coefficient according to the different variables used in the design of the heat exchanger. It is possible to know the preference for changing the design of the heat exchanger when calculating the highest cycle performance coefficient.

Table 9: The exit temperatures of the heat exchanger and the performance coefficient according to the variables used in the design of the heat exchanger.

Tube dimeter (mm)	Number of tubes	Length pipe (mm)	Outlet cold temperature (°C)	Outlet hot temperature (°C)	COP
4	9	150	3.98	33.08	4.452
4	9	225	5.26	23.59	5.001
4	9	300	5.24	20.77	5.127
4	13	150	4.47	28.67	4.699
4	13	225	5.92	20.44	5.206
4	13	300	5.89	18.00	5.314
4	17	150	4.97	22.05	5.044
4	17	225	6.58	15.73	5.485
4	17	300	6.55	13.84	5.566
6	17	150	3.69	23.57	4.864
6	17	225	6.41	21.52	5.204
6	17	300	6.77	21.50	5.24

4. Conclusions

Where the results obtained from the simulation programs will be summarized in detail:

1. The measurement of the intensity exchanger for the produced tubes fundamentally affects the refrigeration worth of the gas coming from the condenser, which has moderately high temperatures. As the state of the cycle fluctuates as per the breadth of lines, and point 4 expanded altogether through the worth of temperature and entropy. The case was 4 mm better contrasted with 6 mm pipe measurement. This can be

affirmed by the COP esteem to 5.566, which builds the productivity of the cooling framework.

2. The length of the intensity exchanger significantly influences the worth of the leave temperatures and the temperature distinction. For a length of 225 mm, the temperature arrived at 15.73 ℃ and for 300 mm it arrived at 13.847 °C. The critical decrease in temperatures assists with expanding the productivity in the refrigeration cycle. High productivity of cooling in the intensity exchanger seems when the length is 300 mm contrasted with different lengths.
3. The best COP came to is 5.566 for the situation where the length of the intensity exchanger is 300 mm and the width of the cylinders is 4 mm. The worth of hot temperatures diminishes emphatically with an expansion in the length, and the contrary way of behaving for the virus side. Concerning the line measurement of 6 mm notice similar highlights, that is to say, the expansion in size diminishes the worth of the leave temperatures for the hot side.

References

[1] Sumeru, T.P. Pramudantoro, F.N. Ani, H. Nasution, Enhancing Air Conditioning Performance Using TiO_2 Nanoparticles in Compressor Lubricant, Adv. Mater. Res. 1125 (2015) 556–560. https://doi.org/10.4028/www.scientific.net/amr.1125.556.

[2] R.I. Tritjahjono, K. Sumeru, A. Setyawan, M.F. Sukri, Evaluation of Subcooling with liquid-suction heat exchanger on the performance of air conditioning system using R22/R410A/R290/R32 as refrigerants, J. Adv. Res. Fluid Mech. Therm. Sci. 55 (2019) 1–11.

[3] K. Sumeru, C. Sunardi, M.F. Sukri, Effect of compressor discharge cooling using condensate on performance of residential air conditioning system, AIP Conf. Proc. 2001 (2018). https://doi.org/10.1063/1.5049962.

[4] S. Choi, U. Han, H. Cho, H. Lee, Review: Recent advances in household refrigerator cycle technologies, Appl. Therm. Eng. 132 (2018) 560–574. https://doi.org/10.1016/j.applthermaleng.2017.12.133.

[5] V. Pérez-García, J.M. Belman-Flores, J.L. Rodríguez-Muñoz, V.H. Rangel-Hernández, A. Gallegos-Muñoz, Second law analysis of a mobile air conditioning system with internal heat exchanger using low GWP refrigerants, Entropy. 19 (2017). https://doi.org/10.3390/e19040175.

[6] S. Qian, J. Yu, G. Yan, A review of regenerative heat exchange methods for various cooling technologies, Renew. Sustain. Energy Rev. 69 (2017) 535–550. https://doi.org/10.1016/j.rser.2016.11.180.

[7] J.F. Ituna-Yudonago, J.M. Belman-Flores, F. Elizalde-Blancas, O. García-Valladares, Numerical investigation of CO2 behavior in the internal heat exchanger under variable boundary conditions of the transcritical refrigeration system, Appl. Therm. Eng. 115 (2017) 1063–1078. https://doi.org/10.1016/j.applthermaleng.2017.01.042.

[8] A. Mota-Babiloni, J. Navarro-Esbrí, J.M. Mendoza-Miranda, B. Peris, Experimental evaluation of system modifications to increase R1234ze(E) cooling capacity, Appl. Therm. Eng. 111 (2017) 786–792. https://doi.org/10.1016/j.applthermaleng.2016.09.175.

[9] J.M. Belman-Flores, A.P. Rodríguez-Muñoz, C.G. Pérez-Reguera, A. Mota-Babiloni, Étude expérimentale sur le remplacement immédiat du R134A par du R1234yf dans un réfrigérateur domestique, Int. J. Refrig. 81 (2017) 1–11. https://doi.org/10.1016/j.ijrefrig.2017.05.003.

[10] Prayudi, R. Nurhasanah, R.A. Diantari, The effect the effectiveness of the liquid suction heat exchanger to performance of cold storage with refrigerant R22, R404A and R290/R600a, AIP Conf. Proc. 1788 (2017). https://doi.org/10.1063/1.4968320.

[11] H. Cho, C. Park, Experimental investigation of performance and exergy analysis of automotive air conditioning systems using refrigerant R1234yf at various compressor speeds, Appl. Therm. Eng. 101 (2016) 30–37. https://doi.org/10.1016/j.applthermaleng.2016.01.153.

[12] A. Mota-Babiloni, J. Navarro-Esbrí, F. Molés, Á.B. Cervera, B. Peris, G. Verdú, A review of refrigerant R1234ze(E) recent investigations, Appl. Therm. Eng. 95 (2016) 211–222. https://doi.org/10.1016/j.applthermaleng.2015.09.055.

[13] G. Pottker, P. Hrnjak, Effect of the condenser subcooling on the performance of vapor compression systems, Int. J. Refrig. 50 (2015) 156–164. https://doi.org/10.1016/j.ijrefrig.2014.11.003.

[14] M.F. Sukri, M.N. Musa, M.Y. Senawi, H. Nasution, Achieving a better energy-efficient automotive air-

conditioning system: a review of potential technologies and strategies for vapor compression refrigeration cycle, Energy Effic. 8 (2015) 1201–1229. https://doi.org/10.1007/s12053-015-9389-4.

[15] M. Ramadan, M.G. El Rab, M. Khaled, Parametric analysis of air-water heat recovery concept applied to HVAC systems: Effect of mass flow rates, Case Stud. Therm. Eng. 6 (2015) 61–68. https://doi.org/10.1016/j.csite.2015.06.001.

[16] Z. Qi, Performance improvement potentials of R1234yf mobile air conditioning system, Int. J. Refrig. 58 (2015) 35–40. https://doi.org/10.1016/j.ijrefrig.2015.03.019.

[17] M. Xing, R. Wang, J. Yu, Application of fullerene C60 nano-oil for performance enhancement of domestic refrigerator compressors, Int. J. Refrig. 40 (2014) 398–403. https://doi.org/10.1016/j.ijrefrig.2013.12.004.

[18] K. Sumeru, S. Sulaimon, H. Nasution, F.N. Ani, Numerical and experimental study of an ejector as an expansion device in split-type air conditioner for energy savings, Energy Build. 79 (2014) 98–105.https://doi.org/10.1016/j.enbuild.2014.04.043.

[19] A. Mota-Babiloni, J. Navarro-Esbrí, Á. Barragán, F. Molés, B. Peris, Drop-in energy performance evaluation of R1234yf and R1234ze(E) in a vapor compression system as R134a replacements, Appl. Therm. Eng. 71 (2014) 259–265. https://doi.org/10.1016/j.applthermaleng.2014.06.056.

[20] K. Sumeru, H. Nasution, F.N. Ani, Numerical study of ejector as an expansion device in split-type air conditioner, Appl. Mech. Mater. 388 (2013) 101–105. https://doi.org/10.4028/www.scientific.net/AMM.388.101.

[21] Krishna, Akshay Bharadwaj, et al. "Technoeconomic Optimization of Superalloy Supercritical CO2 Microtube Shell-And-Tube-Heat Exchangers." Applied Thermal Engineering, vol. 220, Feb. 2023, p. 119578, doi:https://doi.org/10.1016/j.applthermaleng.2022.119578.

[22] Khan, Abdullah, et al. "Numerical and Experimental Analysis of Shell and Tube Heat Exchanger with Round and Hexagonal Tubes." Energies, vol. 16, no. 2, Jan. 2023, p. 880, doi:https://doi.org/10.3390/en16020880.

[23] "Ansys | Engineering Simulation Software." www.ansys.com, ansys.com.